Available online at www.sciencedirect.com
SCIENCE DIRECT®
Infrared Physics & Technology 44 (2003) 527–532
INFRARED PHYSICS & TECHNOLOGY
www.elsevier.com/locate/infrared

InAs/GaAs quantum dot infrared photodetectors with different growth temperatures

S.Y. Wang [a,*], S.C. Chen [b], S.D. Lin [b], C.J. Lin [b], C.P. Lee [b]

[a] *Institute of Astronomy and Astrophysics, Academia Sinica, Taipei 106, Taiwan*
[b] *Department of Electronic Engineering, National Chiao Tung University, HsinChu 300, Taiwan*

Abstract

InAs/GaAs quantum dot infrared photodetectors were fabricated with quantum dots grown at three different temperatures. Large detection wavelength shift (5–14.5 μm) was demonstrated by changing 40 degrees of the epitaxy temperature. The smaller quantum dots grown at lower temperature generate 14.5 μm responses. The detectivity of the normal incident 15 μm QDIP at 77 K is 3×10^8 cm $Hz^{1/2}$/W. A three-color detector was also demonstrated with quantum dots grown at medium temperature. The three-color detection comes from two groups of different sizes of dots within one QD layer. This new type of multicolor detector shows unique temperature tuning behavior that was never reported before.

PACS: 85.60.Gz; 73.50.Pz

Keywords: Quantum dot; Intersubband; Infrared detector

1. Introduction

In the past few years, quantum dot infrared photodetectors (QDIPs) have been widely investigated. The three dimensional confinement of the quantum dot structure provides the possibility to suppress the electron phonon interaction and relax the selection rule of intersubband transition in quantum well structures. Thus, QDIPs are of great potential to overcome the drawbacks of the commercialized QWIPs [1] and become low cost, high temperature operation infrared detectors. The success of the S-K mode QDs fabrication technique accelerates the development of QDIPs. After some pioneering work [2,3], high performance QDIPs were successfully demonstrated with AlGaAs blocking layer in our previous work [4] and also by other groups [5,6]. The AlGaAs barrier decreases the dark current remarkably and enhanced the working temperature of QDIPs.

QDIPs with different detection wavelength were also reported with different material combination. Tuning the absorption wavelength of InAs QDs has been demonstrated using different barrier material [3] and changing the nominal thickness of InAs layer [7]. Multicolor detection QDIP was also demonstrated by stacking different QDs [8]. However, it is noticed that the detection

* Corresponding author.
E-mail address: sywang@asiaa.sinica.edu.tw (S.Y. Wang).

1350-4495/$ - see front matter © 2003 Elsevier B.V. All rights reserved.
doi:10.1016/S1350-4495(03)00164-6

wavelength of the simple InAs/GaAs QD structure varies from different research groups. It indicates that the wavelength tuning and multicolor detection can be achieved by the simple InAs/GaAs structure. It is known that the size and shape of the S-K mode QD can be changed by different epitaxy temperature. At the same time, the influence of growth temperature to the device characteristics is not clear. Therefore, in this work, InAs/GaAs QDIPs with three different growth temperatures were investigated to tailor the detection wavelength. Different detection wavelengths were achieved with identical structures. Three-color detector was demonstrated using single structure with bimodal size distribution of QDs under certain growth temperature.

2. Experiments

The samples were grown by Varian Gen II MBE machine on (1 0 0) GaAs semi-insulating substrate. Ten periods of InAs/GaAs QDs with 500 Å barriers were used in the active region. Each barrier consisted of 470 Å GaAs layer and 30 Å $Al_{0.2}Ga_{0.8}As$ current blocking layer that was supposed to partially cover the quantum dots. The detail function of the current blocking layer was explained in Ref. [9]. The active region was sandwiched by 5000 Å n-type contact layers. δ-doped Si layer with concentration of 1×10^{10} cm^{-2} was inserted 20 Å before each QD layer to supply carriers into QDs. The nominal thickness of InAs QD is 2.6 ML. During the deposition of InAs, a 30 s interruption was added every 0.6 ML InAs deposition. Three different samples were grown at 530 °C (sample A), 510 °C (sample B) and 490 °C (sample C), respectively. After the whole structure was grown, an additional QD layer with the same growth condition as the active region was deposited on the top of the device for the following AFM measurement. The structure is schematically shown in Fig. 1.

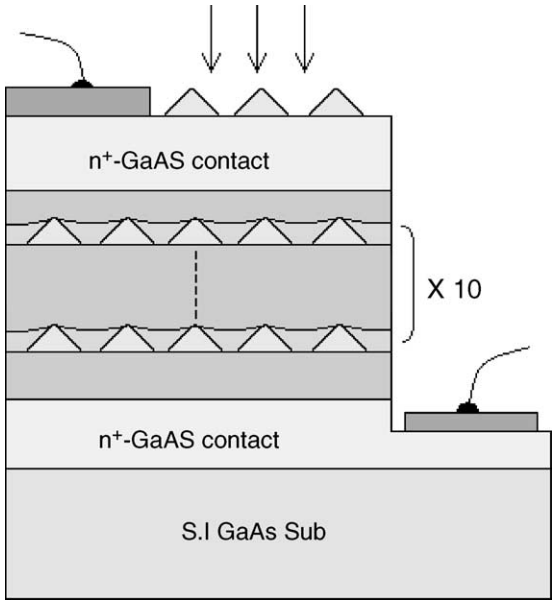

Fig. 1. The schematic diagram of the sample structure.

After the samples were grown, AFM and PL measurements were performed before the device process. Fig. 2 shows the AFM pictures of the

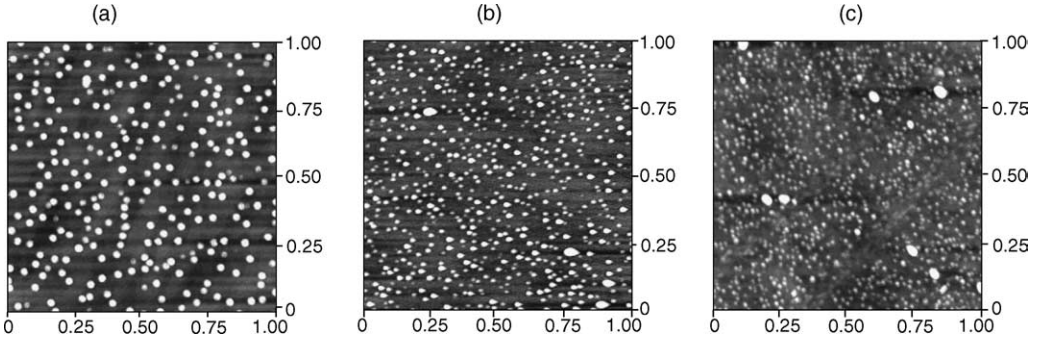

Fig. 2. The AFM pictures of the samples. The scanned area is 1 μm×1 μm.

samples. In sample A, large QDs are formed with regular size of 60 Å in height and 200 Å in radius. The dot density is about 2.5×10^{10} cm^{-2}. As the growth temperature decreases, the QD size shrinks with increasing dot density. The typical QD size of sample C is about 25 Å high and the radius is around 150 Å. The density goes up to 8×10^{10} cm^{-2}. For the medium temperature sample B, bimodal size distributions of QDs were formed. The size of the smaller dots is close to that of sample C with area density of 3.5×10^{10} cm^{-2}, while the large dot height is about 50 Å with 170 Å radius and the density is about 2×10^{10} cm^{-2}. Due to the low growth temperature, the surface roughness increases and some coalescence dots were formed in sample B and C. Also, the uniformity of the size distribution decreases as temperature decreases. The shrinkage of the QD size increases the PL transition energy as we expected. Fig. 3 shows the PL spectrum of the samples at 20 K. The ground state transition energy of sample A is about 1.1 eV, while for sample C, the transition energy increases to 1.18 eV. The relatively broad ground state transition of sample B is consistent with the bimodal QD distribution result from AFM. In addition to the energy shift, the PL intensity decrease for sample B and C. It is consistent with the deteriorated quality of sample B and C as observed in the AFM results.

Standard processing techniques were used to define the mesas and make ohmic contacts. The mesa size is 200 μm×200 μm square. AuGe contact ring is fabricated on mesa top to allow the following normal incident measurement.

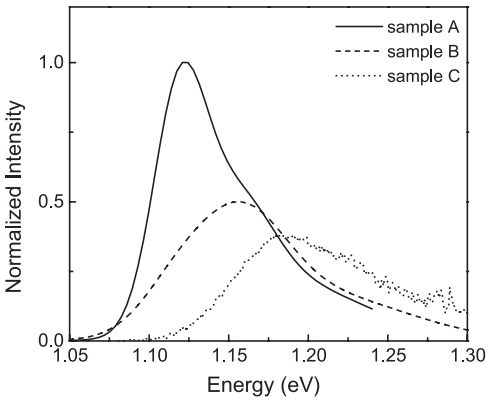

Fig. 3. The PL spectra of the samples at 20 K.

3. Results and discussion

After the devices were fabricated, dark current–voltage (I–V) characteristics at different temperatures were measured using a close cycled helium cryostat. In all the measurements, the bottom contact is referenced as ground. The photoresponse of the devices were measured at different temperatures by a FTIR spectrometer, and calibrated by a 1000 K blackbody source under normal incident illumination. The detailed characteristics of each sample are discussed in following. For simplicity, we will discuss the single wavelength detector sample A and C first and then the multicolor sample B.

3.1. Sample A

The voltage dependence of responsivity and the responsivity spectra of sample A are depicted in Fig. 4. Sample A shows the responsivity peak at

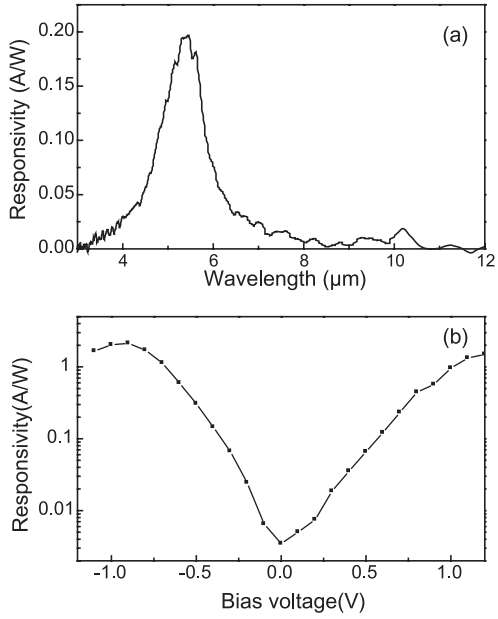

Fig. 4. (a) The responsivity spectrum at 0.7 V and 77 K; (b) the responsivity vs. voltage plot of sample A.

5.5 μm with FWHM about 1 μm. The responsivity increases exponentially with voltage. It comes from the fast increase of current gain and impact ionization. Due to the asymmetric position of AlGaAs barrier, the responsivity is lower under positive biases than negative biases. From the PL measurement with high excitation energy, the wetting layer energy of sample A is about 1.39 eV. The responsivity cutoff energy (206 meV) is coincident with the energy difference between the ground state of the QD to the confined 2D wetting layer state if we assume 70% transition energy is from the conduction band. Under 0.6 V at 77 K, the detectivity is 3×10^9 cm $Hz^{1/2}$/W with responsivity of 0.12 A/W. The BLIP temperature of the device is higher than 64 K for bias less than 0.7 V with 45° FOV. The performance is similar to our previous result.

3.2. Sample C

The responsivity spectrum for sample C at ±1 V, 65 K is shown in Fig. 5. As the growth temperature changes from 530 to 490 °C, the detection energy changes dramatically from 5.5 to 14.5 μm. The narrow FWHM of the response signal ($\Delta\lambda/\lambda = 8\%$) indicates the transition happens between two bound states in the QD. The relatively narrow FWHM may come from the enhanced lateral coupling of the QD due to the high QD density [10]. It was also found that the transition

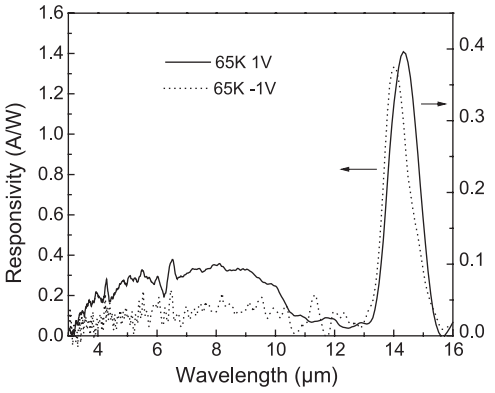

Fig. 5. The responsivity spectrum at ±1 V and 65 K for sample C.

peak shifts under different bias direction. The shift comes from the quantum confined Stark effect due to the asymmetric AlGaAs blocking layer and the bound excited state. In addition to the long wavelength transition, an extended signal in shorter wavelength is found. This broad signal may be from the larger size distribution of the QDs with transitions to wetting layer state. From the blackbody measurement, the photocurrent of sample A is about twice of that of sample C. For all three samples, the doping density is smaller than the QDs density to ensure no excess carrier. Although the QD density is higher in sample C, the effective carrier number is similar for all the samples. This smaller photocurrent is probably due to the deteriorated quality of the QDs and also the lower excited state energy.

It should be noticed that the AlGaAs blocking layer is too thick for sample C because of the smaller QD size. This results in the lower dark current. The dark current at 77 K under 0.5 V (corresponding E-field is 9 kV/cm) is 2.65×10^{-6} A which is about 100 times less than that of typical QWIP with 14 μm cutoff wavelength [1]. Moreover, the detectivity is 3×10^8 cm $Hz^{1/2}$/W at 77 K at −0.6 V and is similar to that of 14 μm QWIPs at the same temperature. The corresponding responsivity is 0.26 A/W and the BLIP temperature is about 55 K for bias under 0.7 V. This is the first long wavelength QDIP that shows comparable performance with QWIPs. Due to the thick AlGaAs layer, the highest detectivity of sample C is reached with negative biases unlike sample A. Compared with sample A, the superior performance of the sample C comes from the narrow response peak due to the high QD density. Further optimizing the AlGaAs blocking layer and increasing the doping density is under investigation to improve the performance.

3.3. Sample B

For sample B, two groups of different sizes of QDs results in three-color detection. As shown in Fig. 6, three detection peaks locate at 5, 9.5, 14.5 μm. The 5 μm peak is relatively broad and comes from the transition in the large dots similar to sample A. The wider size distribution of sample B

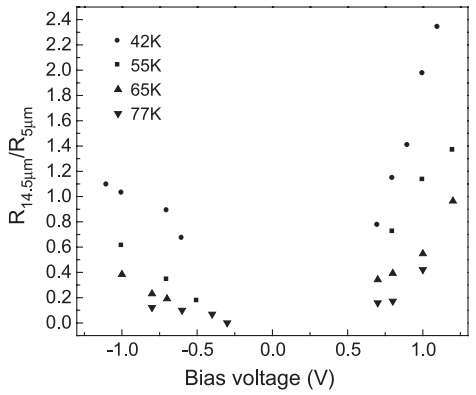

Fig. 6. The responsivity spectrum at ±0.8 V and 65 K for sample B.

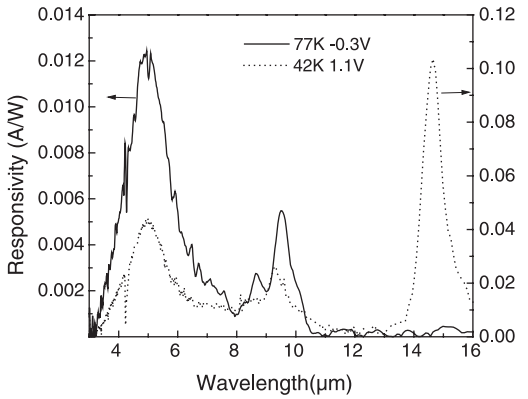

Fig. 7. The responsivity ratio of the 14.5 μm to the 5 μm peak in sample B.

makes the FWHM larger than in sample A. The other two peaks are narrower and come from the bound to bound transition of the large dots (9.5 μm) and the small dots (14.5 μm). Again, the two bound to bound state transitions show wavelength shift due to Stark effect when bias direction changes. The 14.5 μm signal is similar to the peak of sample C. Compared with sample A, the relative small size of the large QD in sample B increases the bound excited state energy and enhances the escape probability of the 9.5 μm signal.

In the reported multicolor detectors, the wavelength tuning signal comes from either different stack of the active region (stacked structure) or inside one quantum structure (coupled or asymmetric well). However, in our sample, the wavelength tuning comes from QDs in the same layer but with different lateral positions. This leads to a unique tuning behavior. The responsivity ratio between 14.5 and 5 μm under different voltages at 42, 55, 65 and 77 K are plotted in Fig. 7. The sample also shows strong temperature tuning behavior. The plot shows a clear trend that the responsivity of the 14.5 μm peak increases as voltage increases and temperature goes down. The voltage tuning behavior comes from the difference of the ground state energy of the QDs. At small biases, the lower ground states of the large QDs are occupied and the population of electrons in the small dots is low. As the voltage increases, the electron number increases and the population in the small QD increases. More obvious tuning behavior is found under positive biases. It is caused by the AlGaAs blocking layer. The 30 Å blocking layer fully covers the small dot while leaves the tip of the large dots uncovered. The 14.5 μm photocarriers need more voltage to escape from the bound excited state. The temperature tuning behavior also comes from the carrier distribution. As the temperature decreases, the number of phonons decreases. It limits the relaxation of carriers into the low energy ground states of the large dots. The lower the temperature, the harder the lower energy state can be supplied. This phonon bottleneck phenomena has also been observed experimentally under unipolar carrier condition [11]. Two extremely tuning spectra are shown in Fig. 8. The

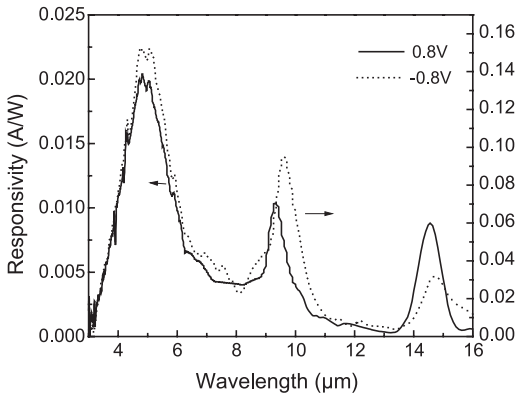

Fig. 8. The normalized responsivity spectrum of sample B at 77 K, −0.3 V and 42 K, 1.1 V.

responsivity ratio of 14.5 and 5 μm is zero at small biases at 77 K and larger than 2 for bias large than 1 V at 42 K. The ratio can be tuned from 0.4 to 2.0 at 1 V when the device temperature decreases from 77 to 42 K. It can also be changed from 0 to 0.7 at 77 K if the voltage increases from −0.3 to 1.2 V. This feature shows the potential of the detector in temperature sensing and other applications.

Due to the wide detection range, the responsivity of sample B is relatively low. The responsivity at 77 K with 0.6 V is 10.3 mA/W for 5 μm peak and 5 mA/W for 9.5 μm peak. The corresponding detectivity is 4×10^8 cm $Hz^{1/2}$/W and 2×10^8 cm $Hz^{1/2}$/W respectively. The highest detectivity for 14.5 μm at 77 K is 7×10^7 cm $Hz^{1/2}$/W. The performance could be improved by increasing the doping concentration and improve the size distribution of the QD.

4. Summary

We have fabricated InAs/GaAs QDIPs with three different growth temperatures. The change of QD size and density resulted in different detection wavelengths and device performance. The high temperature sample showed similar result to our previous data. Low temperature growth process led to the high density of small dots. The device showed low dark current and high performance in very long wavelength. The detectivity is 3×10^8 cm $Hz^{1/2}$/W at 77 K with 55 K BLIP temperature. The performance is comparable with QWIPs of 14 μm cutoff wavelength. The medium temperature sample showed unique three-color detection property. The new temperature and voltage tuning behavior comes from the bimodal size distribution of the QDs within one layer. The long wavelength peak decreases with temperature and increases with voltage. The responsivity ratio of the 14.5 and 5 μm peak can be easily tuning from 0 to larger than 2. The device shows great potential of QDIPs to be used in temperature sensing and other applications. Further optimization of the two devices is under investigation to improve the device characteristics.

Acknowledgement

The work was supported by the National Science Council under contract number NSC91-2112-M-001-044.

References

[1] B.F. Levine, J. Appl. Phys. 74 (1993) R1–R81.
[2] D. Pan, E. Towe, S. Kennerly, Appl. Phys. Lett. 75 (1999) 2719–2721.
[3] J. Phillips, P. Bhattacharya, S.W. Kennerly, D.W. Beekman, M. Dutta, IEEE J. Quantum Electron. 35 (1999) 936–943.
[4] S.Y. Wang, S.D. Lin, H.W. Wu, C.P. Lee, Appl. Phys. Lett. 78 (2001) 1023–1025.
[5] Z. Chen, O. Baklenov, E.T. Kim, I. Mukhametzhanov, J. Tie, A. Madhukar, Z. Ye, C. Campbell, J. Appl. Phys. 89 (2001) 4558–4563.
[6] A.D. Stiff, S. Krishna, P. Bhattacharya, S.W. Kennerly, IEEE J. Quantum Electron. 37 (2001) 1272–1278.
[7] D. Pan, E. Towe, S. Kennerly, M.Y. Kong, Appl. Phys. Lett. 76 (2000) 3537–3539.
[8] Z. Chen, E.T. Kim, A. Madhukar, Appl. Phys. Lett. 20 (2002) 2490–2492.
[9] S.Y. Wang, S.D. Lin, H.W. Wu, C.P. Lee, Infrared Phys. Technol. 42 (2001) 473–477.
[10] C. Mertzner, G.H. Dōhler, Phys. Rev. B 60 (1999) 11005–11013.
[11] J. Urayama, T.B. Norris, J. Singh, P. Battacharya, Phys. Rev. Lett. 86 (2001) 4930–4933.